# Study the Structural and Optical Properties (Energy Gap) of Polythiophene/MWCNT/SnO$_2$ Nanocomposite as an NO$_2$ Gas Sensor

**Faten Adnan Jasim[1a*] and Thamir A. A. Hassan[2b]**

[1]*Department of Physics, College of Science, University of Baghdad, Baghdad, Iraq*
[2]*Department of Physics, College of Science, University of Al-Karkh, Baghdad, Iraq*
[a*] Corresponding author: fatin_adnan90@yahoo.com

## Abstract

Polythiophene (PTh) is very interesting in various applications due to its unique electrical, mechanical and structural properties. In this work, PTh was synthesized using the oxidation method by employing ferric chloride (FeCl$_3$) as an oxidizing agent, Then the nanocomposite polythiophene: Multi-walled carbon nanotubes: Tin (IV) oxide (PTh/MWCNT/SnO$_2$) was prepared by adding constant weight ratio of MWCNT (0.7g) and different weight ratios of SnO$_2$ (0.1, and 0.5g) using the oxidation method. The FE-SEM images of the pure PTh and the nanocomposite showed an apparent change in the morphological composition of the surface. The X-ray diffraction (XRD) pattern of PTh/ MWCNT/SnO$_2$ nanocomposites shows clear peaks for SnO$_2$, while there are broad peaks for MWCNT. As for the polymer, its behaviour is random. The morphology of these nanocomposites shows that the nanotubes were not well aligned and were randomly entangled. The Fourier transformer infrared (FT-IR) spectra of the pure and nanocomposite samples prepared by chemical method in the range of 450-4000 cm$^{-1}$ wave number are recognized as the chemical pledges (bonds) and functional groups in the compound. The band gap energy decreased from 3.53 to 2.78 and 2.97 when SnO$_2$ was added. The sensitivity of the two nanocomposites shows a good enhancement of 14.6% and 62% at the temperature 150$^\circ$C as gas sensor.

## 1. Introduction

Conducting polymers are electrically and ionic conducting polymers [1]. Ionic conducting polymers are usually called polymer electrolytes. Electronically conducting polymers can include conjugated conducting polymers and insulating polymers blending with conducting materials [2-4]. Conducting polymers such as polythiophenes (PThs) have received much attention because of their potential applications including chemical and biological sensors, electronic devices and efficient and low-cost solar cells, due to their remarkable mechanical and electrical properties such as low operating temperature, low cost, flexibility and easy process ability and so on [5, 6]. PThs are polymerized thiophenes, a sulfur heterocyclic. The parent PTh is an insoluble colored solid with the formula (C$_4$H$_2$S)$_n$ [7].

Tin (IV) oxide is an inorganic compound with the formula SnO$_2$ [8]. Multi-wall carbon nanotubes are an important class of technological materials that has numerous novel and useful properties. PTh/MWCNT/SnO$_2$ nanocomposite gives the best results to use in many applications [9-13]. The chemical sensors based on inorganic metal oxides like SnO$_2$ has long been studied for detecting various gases, because of his simple preparation and stability [14].

A chemical sensor comprises of a transducer and an active layer for converting the chemical information into another form of electronic signal like frequency change, current change or voltage change [15]. Therefore, PThs nanocomposite can be used as a Nitrogen dioxide (NO$_2$) gas sensor. NO$_2$ detection is critical because NO$_2$ is a typical toxic gas that is harmful to humans as well as the environment [16]. The purpose of this work is to study the structural and optical properties of polythiophene nanocomposites.

## 2. Experimental Work

PTh was prepared from thiophenes monomer at room temperature by a chemical method. Firstly, 1 ml of thiophene monomer was mixed with 35 ml of chloroform $CHCl_3$. Secondly, 3.7 g of iron chloride $FeCl_3$ was dissolved in 90 ml of chloroform $CHCl_3$. The results were mixed with 0.7g MWCNTs and different concentrations (0.5 and 0.1g) of $SnO_2$. For homogeneity, the solution is placed on magnetic stirrer at a rotational speed of 500 to 1000 RPM. The nanocomposites were filtered and dried to make a powder. Two nanocomposites of 0.9 g polythiophene reinforced with 0.7g MWCNTs and two concentrations (0.1, 0.5) g of $SnO_2$ were prepared by the chemical method. Different techniques including field effect scanning electron microscopic (FE-SEM), X-ray Diffraction (XRD), Fourier transformer infrared (FTIR), and UV-visible) were used to characterize the pure PTh and the two nanostructure composite used in this work. $NO_2$ gas sensors were fabricated from the two nanostructures.

## 3. Results and Discussion

The FE-SEM images of the pure PTh and the nanocomposite (0.9g PTh/0.7g MWCNT/(0.5g,0.1g)$SnO_2$ showed an apparent change in the morphological composition of the surface, as shown in Figs. 1 and 2. The random distribution of $SnO_2$ and MWCNTs was observed. Moreover, the cluster structure of 0.9g PTh/0.7g MWCNT/0.5g $SnO_2$ had an average diameter of 57.54 nm. The FE-SEM image of the nanocomposites 0.9g PTh/0.7g MWCNT/0.1g $SnO_2$ showed a rope-like structure that include nanocomposite [17].
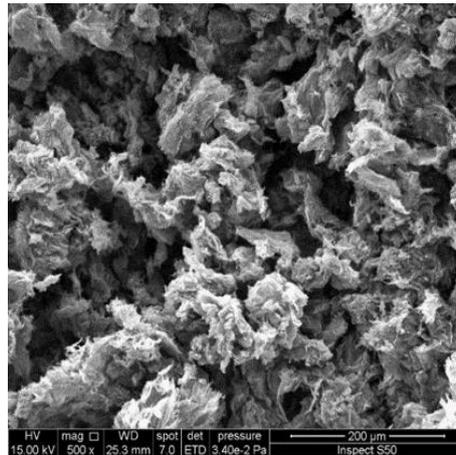


*Figure 1:  FE-SEM of pure PTh.*
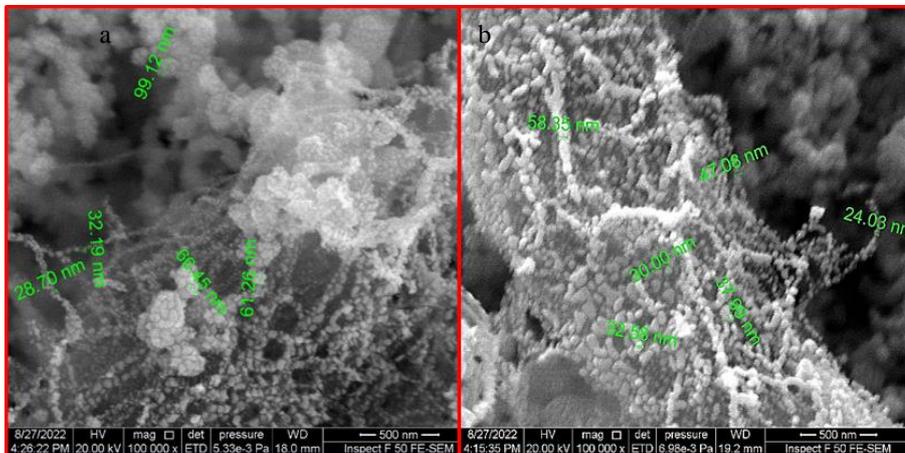


*Figure 2:  FE-SEM images of: a) 0.9g PTh/0.7g MWCNT/0.5g $SnO_2$, b) 0.9g PTh/0.7g MWCNT/0.1g $SnO_2$.*

Figs. 3 and 4 show the XRD patterns of the nanocomposites. The sharp and clear peaks of $SnO_2$ are noted; some of the peaks disappeared as the concentration of $SnO_2$ was decreased [18]. The MWCNTs had broad and overlapping peaks at (002). The XRD characterization of these patterns is listed in Tables 1, 2.
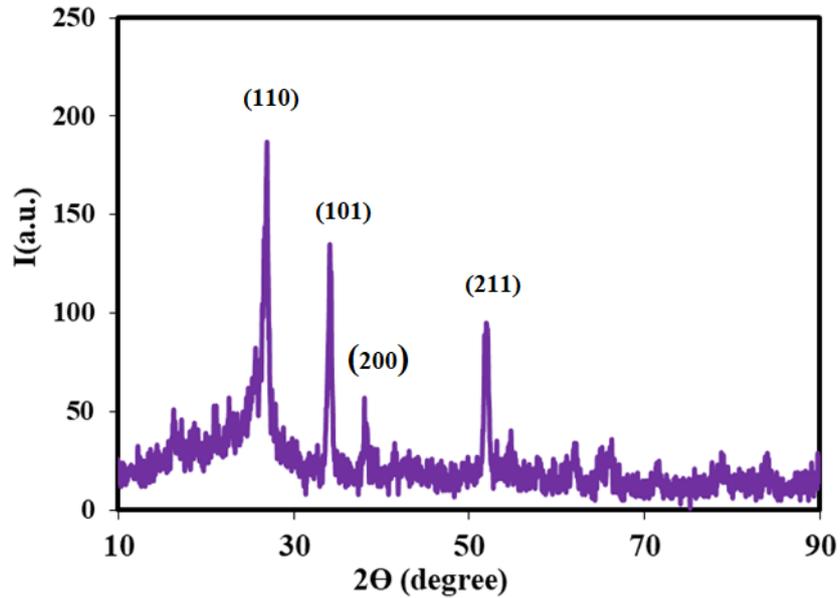


*Figure 3: XRD pattern of the nanocomposite 0.9g PTh/0.7g MWCNT/0.5g SnO₂.*
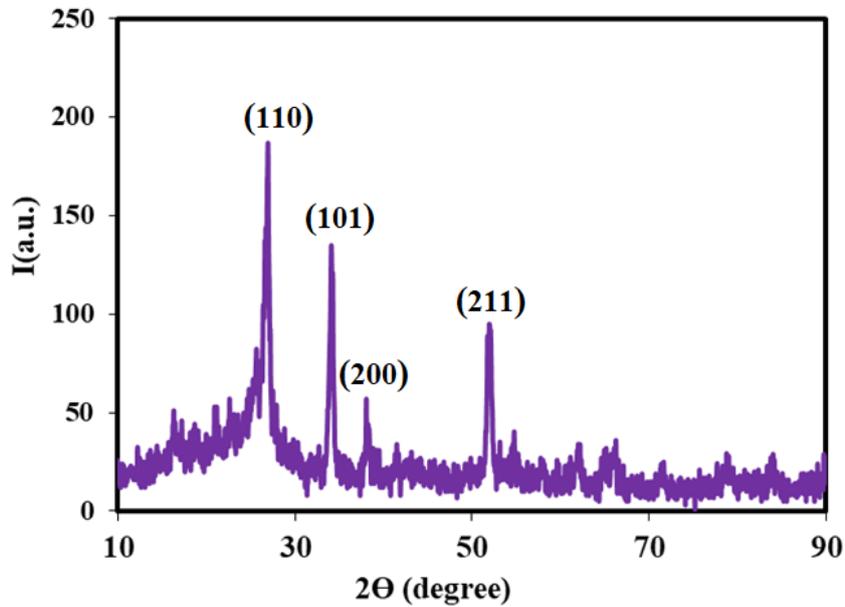


*Figure 4: XRD pattern of the nanocomposite 0.9g PTh/0.7g MWCNT/0.1g SnO₂.*

*Table 1: XRD characterization for 0.9g PTh/0.7g MWCNT/0.5g SnO₂.*

| Sample | 2θ (Deg.) | d hkl Exp.(Å) | hkl | FWHM (Deg.) | C.S (nm) |
|---|---|---|---|---|---|
|  | 26.5 | 3.35 | (110) | 0.36 | 22 |
|  | 33.8 | 2.64 | (101) | 0.34 | 24 |
|  | 37.8 | 2.37 | (200) | 0.34 | 24 |
| 0.9g PTh/0.7g | 51.7 | 1.76 | (211) | 0.38 | 22 |
| MWCNT/0.5g | 54.7 | 1.67 | (220) | 0.39 | 22 |
| SnO₂) | 61.8 | 1.49 | (310) | 0.49 | 18 |
|  | 65.9 | 1.41 | (301) | 0.45 | 20 |
|  | 71.1 | 1.32 | (202) | 0.42 | 23 |

*Table 2: XRD characterization for 0.9g PTh/0.7g MWCNT/0.1g SnO₂.*

| Sample | 2θ(Deg.) | d hkl Exp.(Å) | hkl | FWHM (Deg.) | C.S (nm) |
|---|---|---|---|---|---|
| 0.9g PTh/0.7g MWCNT/0.1g SnO₂ | 26.9 | 3.30 | (110) | 0.44 | 18 |
| | 34.0 | 2.62 | (101) | 0.39 | 21 |
| | 38.2 | 2.35 | (200) | 0.20 | 42 |
| | 51.9 | 1.75 | (211) | 0.37 | 23 |

The Fourier Transform Infrared spectroscopy (FTIR) is a characterization technique used to identify the functional groups in compounds. The FT-IR spectrum in the range of 450-4000 cm$^{-1}$ wavenumber of the individual PTh and PTh/MWCNT/SnO₂ nanocomposite prepared by chemical method, shown in Fig. 5, recognizes the chemical bonds and the functional groups in the nanocomposite [19], as listed in Table 3.

*Table 3: FTIR for pure PTh and PTh/MWCNT/SnO₂ nanocomposites.*

| Samples | Wavenumber (cm$^{-1}$) | Type of band |
|---|---|---|
| PTh | 3446 | O-H |
| | 2925 | C-H |
| | 789 | C-S-H |
| | 1119 | C-S-C |
| | 1664 | C=C |
| 0.9g PTh/0.7g MWCNT/0.5g SnO₂ | 3429 | O-H |
| | 511,457 | Sn=O |
| | 1427 | C-H |
| | 1574 | C=C |
| 0.9g PTh/0.7g MWCNT/0.1g SnO₂ | 3423 | O-H |
| | 514, 468 | Sn=O |
| | 1419 | C-H |
| | 1575 | C=C |
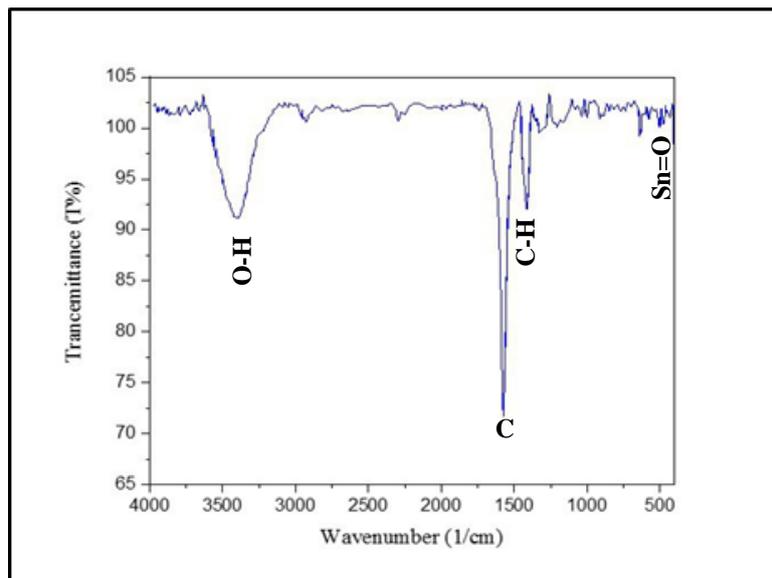


*Figure 5: FTIR spectrum PTh and PTh/MWCNT/SnO₂ nanocomposite.*

Bandgap energy was calculated using Tauc's relation by plotting the relation $(\alpha h\upsilon)^2$ versus photon energy $(h\upsilon)$ and selecting the optimum linear part. Fig. 6 shows the graph of $(\alpha h\upsilon)^2$ as a function of $(h\upsilon)$ for the pure PTh. From this graph, the bandgap energy was found to be about 3.53 eV [20]. The bandgap energy depends on the size and crystallite related to the confinement effect. The bandgap energies for the nanocomposite 0.9g PTh/0.7g MWCNT/0.5g $SnO_2$ was 2.78 eV, and for 0.9g PTh/0.7g MWCNT/0.1g $SnO_2$ was 2.97eV [8, 21]. The band gap energy decreased when $SnO_2$ was added, meaning that the band gap has narrowed and the conductivity increased [22]. Because the distance between the valence band and the conduction band was reduced, it became easier for the electrons to transfer.
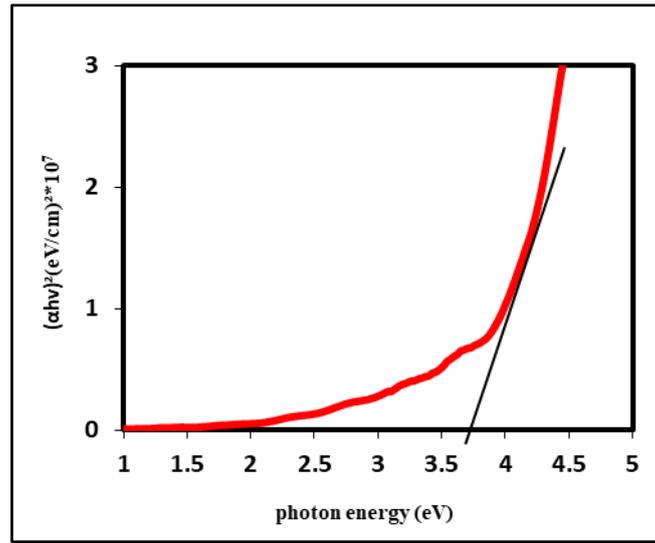


*Figure6:  Tauc's plot of pure PTh.*
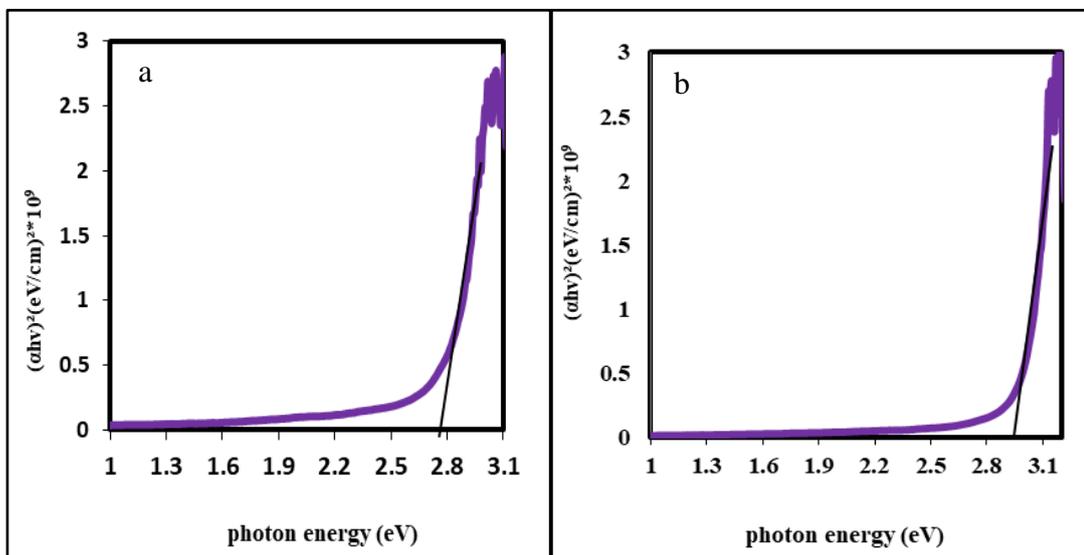


*Figure7:  Tauc's plot of (a) 0.9g PTh/0.7g MWCNT/0.5g SnO₂ and (b) 0.9g PTh/0.7g MWCNT/0.1g SnO₂.*

The pure PTh and the two nanocomposites 0.9gPTh/0.7g MWCNT/0.5g $SnO_2$ and 0.9g PTh/0.7g MWCNT/0.1g $SnO_2$ were used in the fabrication of the $NO_2$ gas sensor. The variations of their resistance with time as a result of gas flow are illustrated in Figs. 8 and 9 in gas-on and gas-off cases, with different temperatures of RT, 100, 150, and 200ºC. The performance is interpreted as the p-type sensor behavior, where, as the

oxidation gas is adsorbed on the sensor surface, it captures some electrons, causing the reduction of its resistance [23].
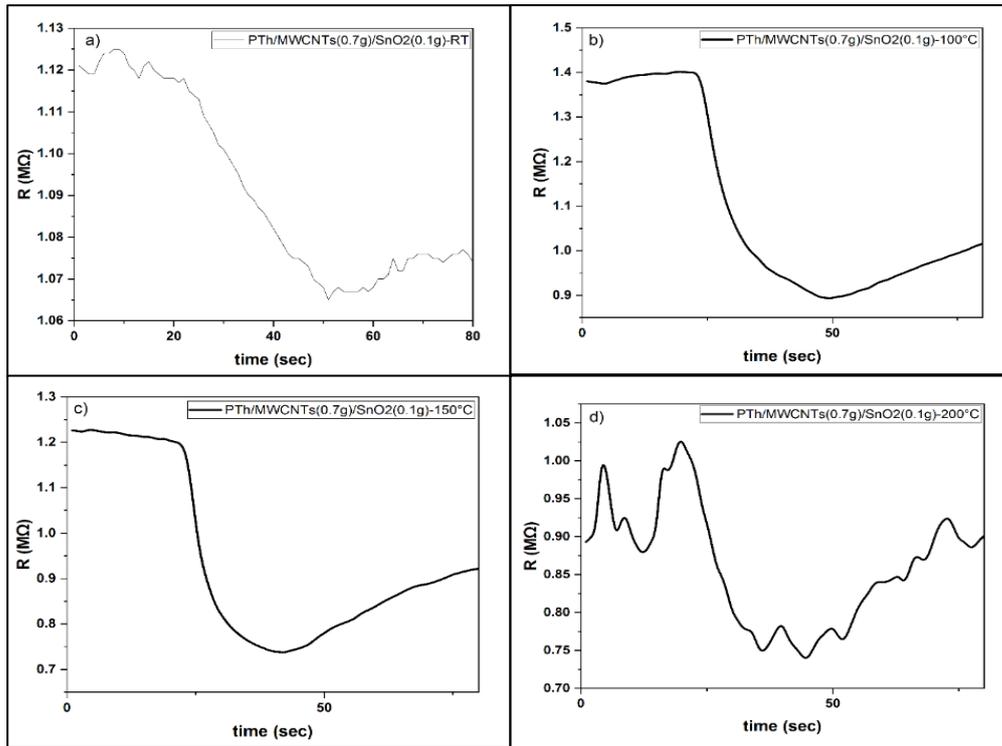


***Figure 8: Resistance variation vs exposure time to NO₂ gas of 0.9g PTh/ 0.7g MWCNT/ 0.1g SnO₂ thin films at(a) RT, (b) 100 •C, (c) 150 •C and (d) 200 •C operating temperatures.***
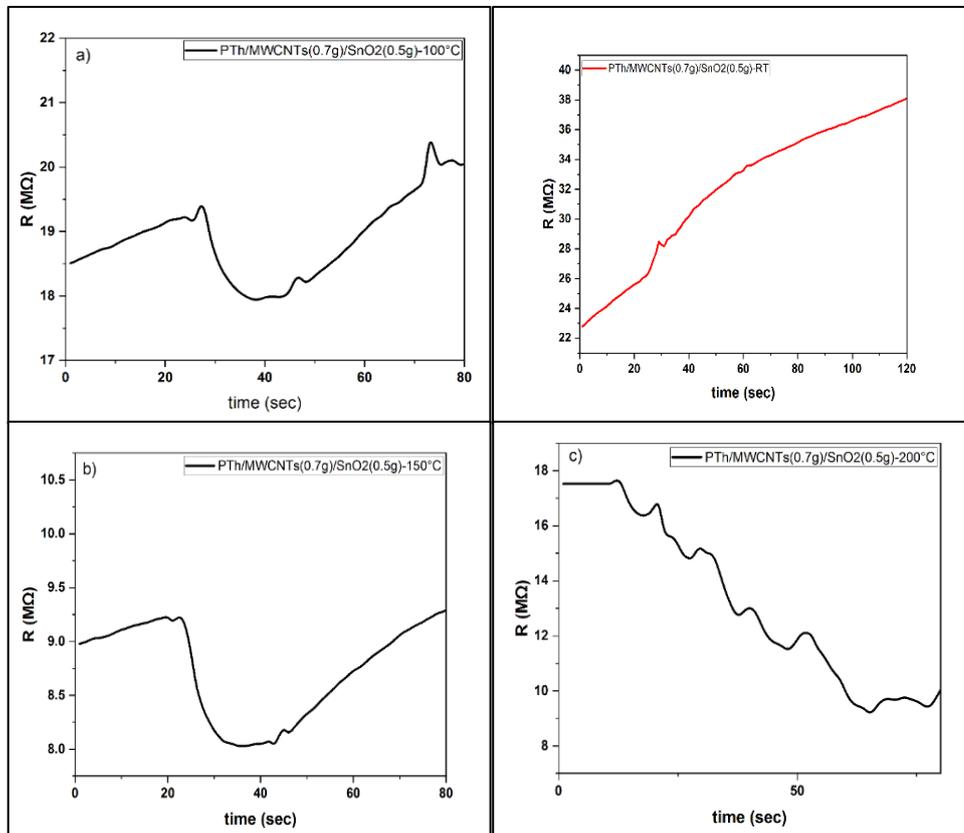


***Figure 9: Resistance variation vs exposure time to NO₂ gas of 0.9g PTh/ 0.7g MWCNT/ 0.5g SnO₂ thin films at (a) RT, (b) 100 •C, (c) 150 •C and (d) 200 •C operating temperatures.***

The sensitivity of the two nanocomposites as a function of applied temperature in the range of $25^{o}C$-$200^{o}C$ for $NO_2$ gas sensors is shown in Fig.10. The highest sensitivity value was 14.6% and 62% at temperature $150C^{o}$ for 0.9g PTh/ 0.7g MWCNT/ 0.5g $SnO_2$ and 0.9g PTh/ 0.7g MWCNT/ 0.1g $SnO_2$, respectively [2].
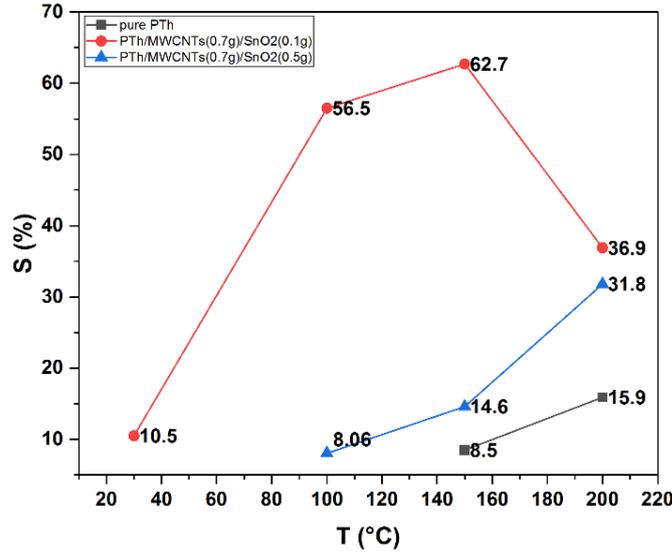


***Fig.10 The sensitivity as a function of the operating temperature for pure PTh, 0.9g PTh/0.7g MWCNT/ 0.1g SnO₂ and 0.9g PTh/ 0.7g MWCNT/ 0.5g SnO₂ fabricated sensors.***

The response and recovery time decreased and increased in relation to the operation temperature. The shortest response and recovery time at this point were for the smallest grain size compared to other samples. The response and recovery time were reduced with the increased oxygen content [24, 25].
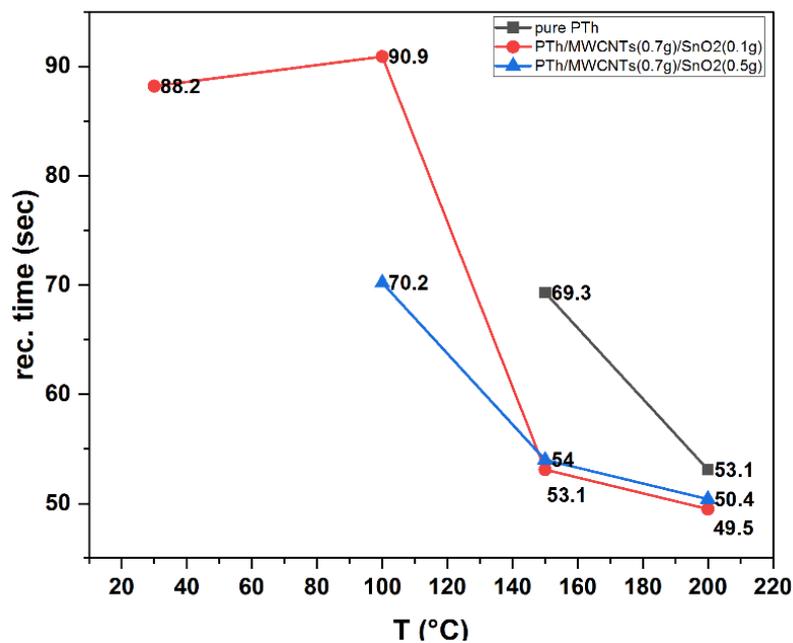


***Figure 11: The recovery time as a function of the operating temperature for pure PTh, 0.9g PTh/ 0.7g MWCNT/ 0.1g SnO₂ and 0.9g PTh/ 0.7g MWCNT/ 0.5g SnO₂ fabricated sensors.***
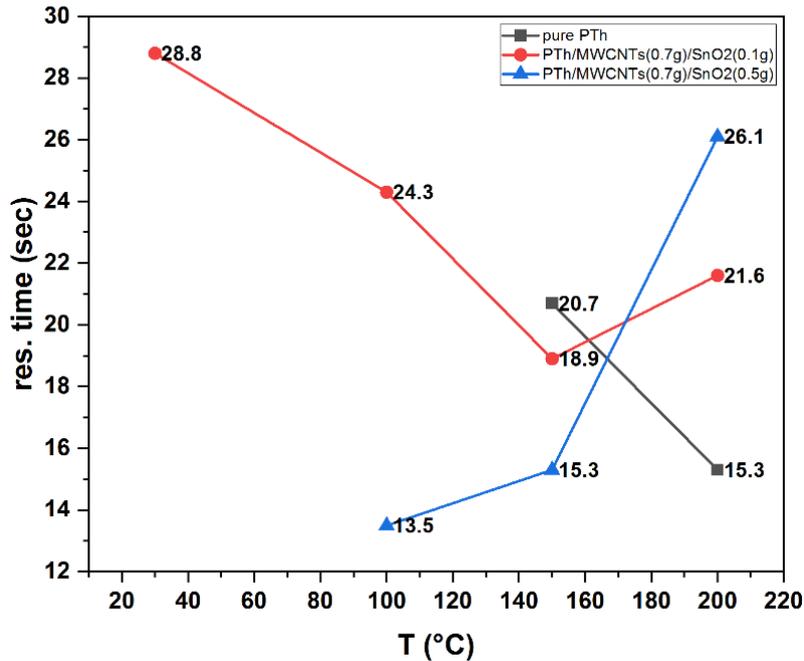
*Figure 12: The response time as a function of the operating temperature for pure PTh, 0.9g PTh/ 0.7g MWCNT/ 0.1g SnO$_2$ and 0.9g PTh/ 0.7g MWCNT/ 0.5g SnO$_2$ fabricated sensors.*

## 4. Conclusions

In this work, the preparation methods are more suitable and easier compared with other methods for composite nanomaterial preparation. The effect of MWCNTs of polythiophene composite may be considered as a major to gas sensors process. The effect of the MWCNTs was noted to be greater than SnO$_2$. This supported the result of the no change in sensitivity as SnO$_2$ was increased. The novelty result of gas sensors appeared at the pattern MS71 which have the sensitivity 10% at room temperature. Finally, PTh nanocomposite recorded more sensitivity compared with individual PTh especially with the multilayer composite.

## Conflict of interest

Authors declare that they have no conflict of interest.

## References

1. A. K. Mishra, J. Atom., Molec. Cond. Nano Phys. **5**, 159 (2018). DOI: 10.26713/jamcnp.v5i2.842.
2. W. R. Saleh, S. M. Hassan, S. Y. Al-Dabagh, and M. A. Marwa, Nano Hyb. Comp. **33**, 93 (2021). DOI: 10.4028/www.scientific.net/NHC.33.93.
3. S. A. Kamal, M. a. L. Jaleel, and A. A. Mohsin, Iraqi J. Sci. **60**, 509 (2019). DOI: 10.24996/ijs.2019.60.3.10.
4. A. Y. Taradh and W. R. Saleh, Nano Hyb. Comp. **36**, 21 (2022). DOI: 10.4028/p-zyn5k5.
5. H. F. Al-Taay, Iraqi J. Sci. **58**, 454 (2022).
6. H. H. Nayel and H. S. "Al-Jumaili", Iraqi J. Sci. **61**, 772 (2020). DOI: 10.24996/ijs.2020.61.4.9.
7. A. Husain, S. Ahmad, and F. Mohammad, Materialia **14**, 100868 (2020). DOI: 10.1016/j.mtla.2020.100868.
8. Z. Huang, J. Zhu, Y. Hu, Y. Zhu, G. Zhu, L. Hu, Y. Zi, and W. Huang, Nanomaterials **12**, 632 (2022). DOI: 10.3390/nano12040632.
9. N. M. Al-Makram and W. R. Saleh, Iraqi J. Sci. **62**, 2543 (2021). DOI: 10.24996/ijs.2021.62.8.7.
10. S. A. Khalaf and I. M. Ali, Iraqi J. Sci. **59**, 2242 (2018). DOI: 10.24996/ijs.2018.59.4C.11.
11. S. M. Omran, E. T. Abdullah, and O. A. Al-Zuhairi, Iraqi J. Phys. **19**, 1 (2021). DOI: 10.30723/ijp.v19i51.691.
12. J. A. Ghafil and M. T. Flieh, Iraqi J. Sci. **63**, 449 (2022). DOI: 10.24996/ijs.2022.63.2.3.

13. R. A. Mohammed and K. A. Saleh, Iraqi J. Sci. **63**, 4163 (2022). DOI: 10.24996/ijs.2022.63.10.3.

14. N. J. Abdullah, A. F. Essa, and S. M. Hasan, Iraqi J. Sci. **62**, 138 (2021). DOI: 10.24996/ijs.2021.62.1.13.

15. H. J. Abdul-Ameer, M. F. Al-Hilli, and F. T. Ibrahim, Iraqi J. Sci. **64**, 630 (2023). DOI: 10.24996/ijs.2023.64.2.12.

16. H. S. Desarkar, P. Kumbhakar, and A. K. Mitra, Mat. Charac. **73**, 158 (2012). DOI: 10.1016/j.matchar.2012.08.014.

17. M. F. A. Alias and H. A. Abdulrahman, Iraqi J. Sci. **62**, 3858 (2021). DOI: 10.24996/ijs.2021.62.11.7.

18. W. A. Al-Taa'y and B. A. Hasan, Iraqi J. Sci. **62**, 4385 (2021). DOI: 10.24996/ijs.2021.62.11(SI).19.

19. E. T. Abdullah and O. A. Ibrahim, Iraqi J. Sci. **62**, 1158 (2021). DOI: 10.24996/ijs.2021.62.4.12.

20. M. Xu, J. Zhang, S. Wang, X. Guo, H. Xia, Y. Wang, S. Zhang, W. Huang, and S. Wu, Sens. Actuat. B Chem. **146**, 8 (2010). DOI: 10.1016/j.snb.2010.01.053.

21. M. A. Abood and B. A. Hasan, Iraqi J. Sci. **64**, 2282 (2023). DOI: 10.24996/ijs.2023.64.5.16.

22. S. Kamat, S. Tamboli, V. Puri, R. Puri, J. Yadav, and O. S. Joo, Arch. Phys. Res. **1**, 119 (2010).

23. S. Thongbor and D. Pattavarakorn, TIChE International Conference ms007 (Hatyai, Songkhla Thailand 2001). p. 1.

24. A. Husain, S. Ahmad, and F. Mohammad, Mat. Chem. Phys. **239**, 122324 (2020). DOI: 10.1016/j.matchemphys.2019.122324.

25. S. Ebrahim, A. Shokry, M. M. A. Khalil, H. Ibrahim, and M. Soliman, Sci. Rep. **10**, 13617 (2020). DOI: 10.1038/s41598-020-70678-8.

# دراسة الخصائص التركيبية والضوئية لمركبات البوليثيوفين *MWCNT/SnO2* النانوية كمتحسس لغاز $NO_2$

**فاتن عدنان جاسم[1] وثامر عبد الامير حسن[2]**

[1] قسم الفيزياء، كلية العلوم، جامعة بغداد، بغداد، العراق

[2] قسم الفيزياء، كلية العلوم، جامعة الكرخ، بغداد، العراق

## الخلاصة

يعد البولي ثيوفين (PThhene) مثيرًا للاهتمام للغاية في مختلف التطبيقات نظرًا لخصائصه الكهربائية والميكانيكية والهيكلية الفريدة. في هذا العمل، تم تصنيع البولي ثيوفين باستخدام طريقة الأكسدة عن طريق استخدام كلوريد الحديديك ($FeCl_3$) كعامل مؤكسد، ثم تم تحضير البولي ثيوفين النانوي المركب النانوي: أنابيب الكربون النانوية متعددة الجدران: تم إعداد أكسيد القصدير ($PTh/MWCNT/SnO_2$) بإضافة نسبة وزن ثابتة من (غم0.7) MWCNT ونسب وزن مختلفة من $SnO_2$ (0.1، و0.5 جم) باستخدام طريقة الأكسدة. أظهرت صور FE-SEM لـ PTh النقي والمركب النانوي تغيرًا واضحًا في التركيب المورفولوجي للسطح. يُظهر نمط حيود الأشعة السينية (XRD) للمركبات النانوية $PTh/ MWCNT/SnO_2$ النانوية قممًا واضحة لـ $SnO_2$، بينما توجد قمم عريضة لـ MWCNT. أما بالنسبة للبوليمر، فإن سلوكه عشوائي. يُظهر مورفولوجيا هذه المركبات النانوية أن الأنابيب النانوية لم تكن متحاذية بشكل جيد وكانت متشابكة بشكل عشوائي. يتم التعرف على أطياف الأشعة تحت الحمراء المحولة فورييه (FT-IR) للعينات النقية والمركبات النانوية المحضرة بالطريقة الكيميائية في نطاق $450\text{-}4000cm^{-1}$، حيث يتم التعرف على التعهدات الكيميائية (الروابط) والمجموعات الوظيفية في المركب. انخفضت طاقة فجوة النطاق من 3.53 إلى 2.78 و2.97 عند إضافة $SnO_2$. تُظهر حساسية المركبين النانويين تعزيزًا جيدًا بنسبة 14.6% و62% عند درجة حرارة 150 درجة مئوية كمستشعر غازات.

**الكلمات المفتاحية:** بولي ثايوفين، مركب نانوي، فجوة الطاقة، زمن الاستجابة، زمن الاسترجاع.